February 1966

LRP 21/66

LABORATOIRE DE RECHERCHES SUR LA PHYSIQUE DES PLASMAS
FINANCÉ PAR LE FONDS NATIONAL SUISSE DE LA RECHERCHE SCIENTIFIQUE

PRESSURE BAR AND PHOTOGRAPHIC MEASUREMENTS ON A HIGH FREQUENCY THETA-DISCHARGE

Ieuan R. Jones

LAUSANNE

February 1966 LRP 21/66

PRESSURE BAR AND PHOTOGRAPHIC MEASUREMENTS ON A HIGH FREQUENCY THETA-DISCHARGE

Ieuan R. Jones

Abstract

A hydrogen plasma is produced by means of a θ-coil which is fed by a high frequency (4.8 Mc/s) generator of 12 Mwatts maximum power. Pressure measurements of the plasma are made by means of the pressure bar technique and a photographic investigation is made with an image converter camera. A tentative description of the gross physical behaviour of the discharge is given.

Lausanne

I INTRODUCTION

Recently, magnetic probe measurements made on a hydrogen plasma produced by means of a high frequency Θ-discharge have been reported 1). The amplitude and phase of the magnetic field which penetrated the interior of the plasma were measured and from the phase-amplitude relationship a determination was made of the propagation vector. This study led to observation of an anomaly in the skin effect which manifested itself when the mean free path for electrons became larger than the skin depth. The measurement of field penetration also permitted a determination of electronic temperatures to be made 2).

A full description of the experimental apparatus used to generate the plasma may be found in Ref. 1. The following is a brief summary of the experimental details. Neutral hydrogen gas contained in a 51 mm diameter, 100 cm long Pyrex discharge tube is preionized by means of a longitudinal discharge. After 20 μsec an alternating magnetic field which is parallel to the axis of the discharge tube is produced by means of a 6 turn coil wrapped around the outside of the tube. The length of this coil is 20 cm. A metallic screen placed between the coil and the discharge tube serves to make the axial field uniform. The frequency of the alternating field is 4.8 Mc/s. The generator is programmed to give an output pulse for which the power increases approximately linearly with time during the first nine cycles. The power delivered at the ninth cycle is about 12 Mwatts.

This report presents the results of pressure measurements and a photographic investigation which were made on this high-frequency discharge in order to elucidate its gross physical behaviour.

II THE PRESSURE MEASUREMENTS

1. The pressure bar gauge

One of the most satisfactory methods of measuring pressures varying on the microsecond time scale is the pressure bar technique. A review of this technique may be found in Ref. 3. In essence the method is as follows. The unknown pressure is applied to one end of a circular cylinder of elastic material. This initiates the propagation of an elastic stress pulse composed of longitudinal waves along the bar. These stress waves traverse a piezoelectric disc cemented into the bar at some station along its length. The charge consequently liberated at the faces of the piezoelectric element is allowed to charge a known capacitance; the voltage developed across this capacitor is observed on an oscilloscope. In this manner the variation of stress with time, and consequently the variation of the applied pressure at an earlier time, may be examined. The acoustic delaying of the pressure signal by the length of the bar between the measuring end and the location of the piezoelectric disc allows one to make pressure measurements in an environment of large electrical interference such as is usually encountered in plasma physics experiments.

The pressure bar used in the present investigation is a circular bar of Pyroceram 9608, a ceramic material marketed by Corning Glass Works, Corning, New York. The diameter of the bar is 0.29 cm and its overall length is 21.0 cm. A PZT-4 polarized ferroelectric disc of 0.30 cm diameter and 0.05 cm thickness is cemented into the bar at a distance of 12.3 cm from the measuring end. Since the bar velocity c_o $(=\sqrt{\frac{E}{\rho}}$, where E is Young's modulus of the bar material and ρ is its density) for Pyroceram 9608 is 0.59 cm/μsec, the stress pulse takes 20.9 μsec to travel from the measuring end to the piezoelectric disc. The recording time of the gauge, that is, the time available for observing the incident stress pulse before its reflection from the remote end of the bar causes interference, is 29.5 μsec.

Fig. 1 shows the location of the pressure bar gauge with respect to the discharge coil; it enters the discharge tube radially, midway along the length of the coil. The design of a suitable housing for a pressure bar always presents problems. Such a housing or seating must satisfy concurrently the following two requirements :

(i) It must allow the unknown pressure to act solely on the end surface of the bar. If the lateral surface of the bar is exposed to the applied pressure, then the gauge will indicate a value of pressure smaller than that which actually obtains.

(ii) In order to avoid distortion of the propagating stress pulse, unrestricted lateral movement of the bar surface must be permitted.

Constructional details of the pressure bar gauge used in this investigation are shown in Fig. 2. The remote end of the pressure bar is cemented into the bottom of an aluminium compartment which supports the electrical connections from the piezoelectric disc to the coaxial cable. The bar is inserted into a glass tube which is closely fitting in the region of the measuring end of the bar but which flares out to a larger radius in the neighbourhood of the piezoelectric element. The ends of the pressure bar and the glass tube are flush; the clearance between the bar and the inner wall of the glass tube is about 0.01 cm. In order to prevent electrical breakdown between the plasma and the piezoelectric element of the gauge, a low pressure ($\sim 10^{-4}$ torr) is maintained within the gauge by means of differential pumping. No problems arising from gas breakdown within the gauge were experienced during this investigation. Parasitic electric fields are screened out by means of a copper sheet wrapped around the outside of the glass tube.

Details of the vacuum seal which permits entry of the gauge into the discharge tube are also shown in Fig. 2. If the large nylon nut, which also provides mechanical support for the pressure gauge, is unscrewed slightly then the gauge may be moved into any desired radial position. Tightening of the nut re-establishes a good vacuum seal.

It should be noted that the pressure bar is not attached to the glass sleeve in any way whatsoever; there is, however, contact between them at a limited number of places. Free lateral movement of the bar surface is, in the main, possible. The other requirement demanded of the seating, namely the isolation of the lateral of the bar from the applied pressure, does not arise in the present application of the pressure bar. The temperature of any plasma that enters the confined region between the glass tube and the bar will certainly be lower than that of the plasma in contact with the measuring end and consequently negligible pressure will be exerted on the lateral surface.

The charge liberated at the faces of the piezoelectric disc develops a voltage across a total capacitance of 546×10^{-12} farads. The capacitative loading of the piezoelectric element was not excessive; it was not found necessary to insert a cathode follower between the element and the coaxial cable which fed the output signal from the gauge to the oscilloscope.

The pressure bar was amplitude calibrated by allowing shock waves of known strength to impinge on the measuring end of the bar. The pressure bar was placed at the closed end of a conventional diaphragm shock tube with its axis parallel to that of the shock tube and with its measuring end flush with the end plate of the shock tube. In such a position the bar measures the excess pressure set up at the end of the expansion chamber on reflection of the incident shock wave. The amplitude sensitivity of the gauge was obtained by comparing the experimental value of the excess

reflection pressure with that computed as follows. Fig. 3 is a schematic representation of the reflection of a shock wave at the closed end of the expansion chamber. Among the equations governing the propagation and normal reflection of plane shock waves in an uniform tube are :

$$\left(\frac{u_1}{a_o}\right)^2 = \frac{(\gamma+1)\ \pi_1 + (\gamma-1)}{2\gamma}$$

and

$$\frac{(\pi_1-1)^2}{\pi_1\ [(\gamma-1)\ \pi_1 + (\gamma+1)]} = \frac{(\pi_2 - 1)^2}{(\gamma+1)\ \pi_2 + (\gamma-1)}$$

where u_1 = speed of the incident shock

a_o = speed of sound in the gas ahead of the incident shock

$\pi_1 = \frac{P_1}{P_o}$; $\pi_2 = \frac{P_2}{P_1}$ where P_j is the pressure in region j

γ = ratio of specific heats

An average value of u_1 over a short distance at the end of the shock tube was found by measuring the time taken by the incident shock to pass two fixed stations. This enables one to calculate the values of both π_1 and π_2 and hence the excess reflected pressure.

$$P_2 - P_o = P_o\ (\pi_1\ \pi_2 - 1)$$

The sensitivity of the pressure gauge used in this study was found to be $1.96 \pm 0.10 \times 10^{-6}$ volt/newton/m^2.

The familiar amplitude-frequency method of specifying the frequency response of a system is only of secondary importance when discussing the behaviour of the pressure bar. The emphasis should rather be put on the time response of the gauge, that is, upon the shape of the output waveform as a function of time for an appropriate input pulse. It is customary to present the response of a system to either a δ-function or a step-function input.

Fig. 4 shows the response of the pressure bar to a step-function pressure input. This data was obtained during the shock tube calibration tests discussed above. The risetime, τ, of the pressure bar (defined as the time taken for the output signal to increase from 10 % to 90 % of its final steady value) is measured to be 0.93 μsec. From pressure bar theory 4, 5) we have that

$$\tau = 1.96 \nu^{2/3} \left(\frac{z_o}{a}\right)^{1/3} \left(\frac{a}{c_o}\right) \qquad \text{(c.g.s. Units)}$$

where ν is Poisson's ratio for the bar material, c_o is the bar velocity, a is the radius of the bar and z_o is the distance along the bar from the measuring end to the point of observation.

For the pressure bar used in this study,

$\nu = 0.25$
$z_o = 12.3$ cm
$a = 0.145$ cm
$c_o = 0.59 \times 10^6$ cm/sec

which yield a theoretical risetime of 0.84 μsec.

From a knowledge of the step-function response of the bar, it is possible to calculate its response to input pulses having various waveforms and risetimes. Such calculations have been

made for sawtooth and triangular shaped input pulses. The results are shown in Figs. 5, 6 and 7. An examination of these graphs leads one to the following conclusion. If the risetime of the input pulse is longer than about 1.5 μsec, then the dispersive oscillations of the bar are reduced to a low level and the output pulse is a fair representation of the input. If, on the other hand, the risetime is faster than 1.5 μsec then dispersive oscillations remain apparent in the output signal even though the total duration of the input pulse may be as long as 3.0 μsec.

2. Pressure bar results.

Pressure-time oscillograms of the discharge were obtained at different radii for filling pressures of 16.5, 30, 60 and 107 mTorr of hydrogen. At each filling pressure, between 30 and 40 radial positions located on a diameter (51 mm) of the discharge tube were sampled. An examination of these oscillograms showed that each one possessed certain characteristics which enabled it to be classified into one of three groups. It was further found that each group contained only oscillograms obtained within a certain range of radial positions. The limits of the ranges of radial positions which define these groups are approximately as follows :

Group	r(mm)
1	50 - 40
2	40 - 16
3	16 - 0

Note r refers to the distance between the measuring end of the pressure bar and the interior wall of the discharge tube opposite it.

There is no clear cut difference between oscillograms taken at radii which span the group limits. Nevertheless, a general categorization is indeed possible. An example from each group for each of the four filling pressures is shown in Figs. 8 and 9.

The distinguishing features of these pressure oscillograms are the following :

Group 1 : For oscillograms in this group, the signal rises to a maximum value and then falls to zero in a perfectly smooth and regular manner. Except for the 30 mTorr filling pressure case, no signs of dispersive oscillations of the pressure bar can be seen.

Group 2 : The signals in this group of oscillograms show a pulse of about 2.5 - 3 μsec duration which either falls off to a constant level signal of a further 2 μsec duration or else falls to zero before being followed by a second pulse of smaller amplitude. Again, no sign of dispersive oscillation is apparent in these oscillograms.

Group 3 : For these oscillograms, the signal rises to a maximum in about 1.5 μsec which, by reference to Figs. 5, 6 and 7, corresponds to the shortest time in which the pressure bar can respond to a fast-rising pulse. The oscillations which are so obvious in this group of oscillograms can, again by reference to Figs 5, 6 and 7, be identified as dispersive oscillations of the pressure bar.

A discussion of these measurements is deferred until later when they can then be correlated with streak pictures which were taken of the discharge.

III THE PHOTOGRAPHIC INVESTIGATION OF THE DISCHARGE

A photographic investigation of the discharge was undertaken using a frame/streak image converter camera (EL 085/IPP, Garching bei Munchen). Streak photographs were taken of the radial and axial motion of the plasma and, in addition, framing pictures were obtained of the axial flow.

Fig. 10 shows the disposition and dimensions of the slits used in this study. In order to obtain the axial framing pictures, the axial slit was enlarged to form a window. There was sufficient luminosity at all filling pressures for satisfactory radial streak pictures to be obtained. These are shown in Fig. 11. Satisfactory axial streak and framing pictures were, however, only obtained for the 107 mTorr and 60 mTorr filling pressure discharge, the luminosity being much too feeble at the lower pressures. Axial streak and framing pictures taken at 107 mTorr are shown in Fig. 12. The origin of time is taken to be the start of the high-frequency discharge. The corresponding pictures taken at 60 mTorr show exactly the same features.

IV DISCUSSION OF RESULTS

1. Pressure bar measurements.

In an attempt to recover as much information as possible from the pressure bar oscillograms, system analysis methods were applied to the pressure bar signals, the aim being to derive the input to the bar given the output and the impulse response function. The validity of each of the procedures which were devised was tested by application to the known, corresponding, input and output

signals shown in Figs. 5, 6 and 7; the required impulse response function was derived from the step-function response of the system which is shown in Fig. 4. No satisfactory solution to this problem was found. If one represented the impulse response function by something more complex than a single δ-function (which gave an input signal which was merely the output shifted to an earlier time), then the slightest imprecision in reading the initial small values of the impulse response function yielded meaningless results. In consequence, the pressure bar oscillograms have to be interpreted as they stand.

The only conclusion we can derive from a study of the group 3 oscillograms is that the pressure bar experiences, in these radial positions, an applied pressure which changes appreciably in times less than about 1.5 μsec - whence the dispersive oscillations apparent in the output signals. This rapid pressure change is probably associated with an inwardly directed motion of the plasma.

Before proceeding to discuss the oscillograms of groups 1 and 2, we will consider the real problem of establishing the relationsship between the measured pressure and the true plasma pressure. If there is no directed motion of the plasma, then the interpretation of the signals is straightforward since the bar records solely the kinetic pressure of the plasma. Complications arise when mass motion is present. Suppose the flow is directed towards the measuring end of the bar. If the flow is subsonic, then the bar records the sum of the kinetic and dynamic pressures (the stagnation or total pressure).

When the flow becomes supersonic then, provided the flow duration is sufficiently long, a detached bow shock is established ahead of the measuring end of the probe 6). On the stagnation streamline the detached shock is normal and the ratio of the true total pressure to the measured total pressure is given by the following expression 7) :

$$\frac{\text{True total pressure}}{\text{Measured total pressure}} = \left[\left(\frac{2\gamma}{\gamma+1}\right) M^2 - \frac{(\gamma-1)}{(\gamma+1)}\right]^{1/\gamma-1} \left[\frac{1+\frac{(\gamma-1)}{2}M^2}{\frac{(\gamma+1)}{2}M^2}\right]^{-\gamma/\gamma-1}$$

where γ = ratio of specific heats

M = flow Mach number

For $\gamma = 1.6$, the above ratio has the following dependence on M.

M	True total pressure / Measured total pressure
1.00	1.00
1.25	1.01
1.50	1.07
1.75	1.17
2.00	1.32

It is seen from the above table that if the flow Mach number is low ($M < 1.5$), then the jump in stagnation pressure across the detached shock is small and again the bar records essentially the sum of the kinetic and dynamic pressures. In the event of the non-establishment of a bow shock or of flows having $M > 1.5$, it appears that a correct interpretation of the pressure bar signals is impossible without additional detailed knowledge of the flow.

If the mass motion is directed away from the measuring end of the bar then the resulting flow is very complicated and, in general, will be turbulent in the neighbourhood of the measuring end. It then becomes impossible to relate the measured pressure to the true plasma pressure.

The oscillograms of group 1 exhibit no dispersive oscillations. Nevertheless, we cannot consider all these signals to represent the true plasma pressure since, from symmetry considerations and the evidence afforded by the group 3 oscillograms, we must conclude

that mass motion of the plasma away from the measuring end of the pressure bar exists in this radial region. It is however, reasonable to assume that a projection of the pressure bar into the discharge tube of only 1-2 mm will not perturb the plasma flow unduly and that, in this position (r = 48-50 mm), the bar will, for early times at least, measure the kinetic pressure near the wall of the discharge tube. At later times the bar may indeed experience dynamic pressures due to an outward radial expansion of the plasma following the initial inwardly directed motion.

Dispersive oscillations are also absent from the signals of the group 2 oscillograms i.e. the pressure bar, when in this radial region, does not experience pressures which change appreciably in times less than about 1.5 μsec. The presence in this central region of radial shocks or significant dynamic radial motion are consequently precluded. The axial flow out of the coil which undoubtedly develops at later times is parallel to the measuring surface of the pressure bar and consequently does not manifest itself in the output signal. We may reasonably infer that these signals are a fair representation of the kinetic pressure of the plasma in the central region of the discharge tube.

The pressure-time signals obtained at the radial positions r = 49 mm and r = 24 mm, for a filling pressure of 107 mTorr, are shown in Fig. 13 together with the time dependence of the average magnetic pressure of the vacuum magnetic field. The time correspondence between various pressure signals is known; for example, it is obvious from the original oscillograms that there is a delay of about 0.4 μsec between the starts of the r = 49 mm and r = 24 mm signals. However, the time relationship between the start of the pressure signals and the start of the high-frequency discharge is not known. It is reasonable, nevertheless, to make the start of the r = 49 mm pressure signal coincide with the start of the high-frequency current pulse and this has been done in Fig. 13.

For the r = 49 mm case, the plasma kinetic pressure remains smaller than the pressure of the vacuum magnetic field for most of the duration of the discharge. Now the applied magnetic field penetrates a few mms into the plasma and at r = 49 mm there will be a magnetic pressure in addition to the gas pressure. If the sum of the magnetic pressure and the gas pressure is equal to the pressure of the vacuum magnetic field then the plasma is confined by the applied magnetic field. If, on the other hand, this sum exceeds the pressure of the vacuum magnetic field then the plasma is confined by the walls of the discharge tube. The pressure bar signals alone cannot determine whether or not there is magnetic field confinement. However, the fact that the gas pressure is indeed smaller than the vacuum field pressure does permit this possibility to exist.

From Fig. 13 we see that the pressure at the centre of the discharge tube soon exceeds the vacuum field pressure and rises to a value which is approximately four times that of the applied field. Since the oscillograms of group 3 suggest the existence of radial motion, we may assume that this enhancement of pressure is mainly brought about by a transport of material from the neighbourhood of the discharge tube wall to the centre.

Finally we point out that the pressure bar signals have the same characteristic form at all filling pressures. This implies that the gross physical behaviour of the discharge does not differ much from one filling pressure to another in the range 16.5 - 107 mTorr.

2. Correlation of the pressure bar signals with the streak photographs of the discharge.

A time correlation was made, for the case of 60 mTorr filling pressure, between the high-frequency current pulse, the radial streak picture and the pressure bar signal. This is shown in

Fig. 14. The upper diagram shows the envelope of the high-frequency pulse as a function of time. The centre diagram is a schematic representation of the luminosity which is visible in the radial streak photograph shown in Fig. 11 (the 60 mTorr case). The lower diagram is the output signal from the pressure bar when situated at r = 24 mm. The start of the pressure signal has been arbitrarily delayed by 0.4 μsec with respect to the start of the discharge current, in accordance with the procedure adopted for Fig. 13.

From the radial streak picture one sees that the plasma, following an initial inwardly directed motion, expands radially outwards and then, for some reason as yet unexplained, collapses again towards the axis of the discharge tube. The pressure bar records a second pressure pulse which correlates well in time with this second contraction of the plasma. Moreover, an examination of all the pressure bar signals reveals that there is, for the plasma produced in this particular experiment, a good correlation between pressure amplitude and intensity of luminosity as seen on the streak pictures.

3. The axial motion of the plasma.

The axial motion of the plasma can be deduced from axial streak pictures similar to the one shown in Fig. 12. The analysis of such a picture taken at a filling pressure of 60 mTorr is shown in Fig. 15 in the form of an x-t plot. 1.5 μsec after the start of the discharge current, a well defined front (see the frame pictures of Fig. 12) appears at the end of the Θ-coil and travels along in an axial direction with a decreasing velocity. The average velocity of this front over the first 6 cm of its travel after leaving the coil is 1.6 cm/μsec. In view of its speed, its well defined nature and the relatively short spatial extent ($\sim$1.3 cm) of the luminosity behind it, it is reasonable to assume that this front is an ionizing shock driven by the axial expansion of the plasma out of the Θ-coil.

V CONCLUSION

We have now reached a point where, with the aid of the experimental evidence reported herein and with some conjecture, we may give a tentative description of the gross behaviour of the high-frequency Θ-discharge.

If the plasma felt only the average pressure of the applied magnetic field then, provided the magnetic overpressure was sufficiently large, a cylindrical shock would propagate towards the axis of the discharge tube. The amplitude of this shock would increase rapidly due to its convergent nature. Such a motion is not observed (recall that group 2 oscillograms do not indicate rapid changes of pressure). We deduce, therefore, that the plasma feels the instantaneous applied magnetic pressure. At each half period of the discharge a shock wave is propagated inwardly to be followed closely by a rarefaction wave which arises when the magnetic pressure temporarily drops to a low value, that is, blast waves are excited at each half cycle of the discharge current. The effect of the rarefaction wave is to attenuate the shock before it reaches the central region of the discharge tube. Gas is transported from the periphery of the discharge into the central region by each blast wave and the pressure in this region consequently rises. The pressure at the wall of the discharge tube is maintained either by the heating of the gas which remains at the wall or by an influx of impurities into the discharge from the glass wall of the tube.

Following the cessation of the discharge current, there is a radial and axial expansion of the central plasma. For some unexplained reason there is a second radial contraction of the plasma. The axial expansion of the plasma produces an axial ionizing shock which propagates away from the coil region.

ACKNOWLEDGEMENTS

The author would like to express his appreciation to Dr. R. Keller for his encouragement and aid with the measurements, to Dr. F.Troyon for many beneficial discussions and to Mr. H. Ripper for his competent technical assistance throughout the study. This investigation was financed by the Fonds National Suisse de la Recherche Scientifique.

REFERENCES

1. R. Keller, Report No LRP 15/65, Lausanne (March 1965)

2. F. Troyon and R. Keller, Report No LRP 17/65, Lausanne (April 1965)

3. I.R. Jones, Report No TDR-594 (1208-01) TR-3, Aerospace Corporation, El Segundo, Calif. (June 1961)

4. R. Folk et al, J. Acoust. Soc. Am. 30, 552 (1958)

5. R.L. Rosenfeld and J. Miklowitz, J. Appl. Mech. 32, 290 (1965)

6. L. Davies, NPL Aero Report 1098, London (April 1964)

7. H.W. Liepmann and A. Roshko, Elements of Gasdynamics John Wiley and Sons, Inc., New York, 1958, page 148.

Figure Captions

Fig. 1 Schematic diagram of experimental apparatus

Fig. 2 Constructional details of the pressure bar and vacuum seal

Fig. 3 Schematic representation of the reflection of a shock wave at the closed end of a shock tube.

Fig. 4 Response of the pressure bar to step-pressure loading.

Fig. 5 Response of the pressure bar to given input pulses.

Fig. 6 Response of the pressure bar to given input pulses.

Fig. 7 Response of the pressure bar to given input pulses.

Fig. 8 Examples of pressure bar signals (Sweep Speed : 1 μsec/div)

Fig. 9 Examples of pressure bar signals (Sweep Speed : 1 μsec/div)

Fig. 10 The disposition and dimensions of the slits used in the photographic study.

Fig. 11 Streak pictures of the radial motion of the plasma.

Fig. 12 Streak and frame photographs of the axial motion of the plasma.

Fig. 13 Comparison of measured pressures with the average pressure of the applied magnetic field.

Fig. 14 Time correlation of the high-frequency pulse, the radial streak picture and the pressure bar signal.

Fig. 15 x-t plot of the axial motion of the plasma; $P_{(filling)} = 60$ mTorr.

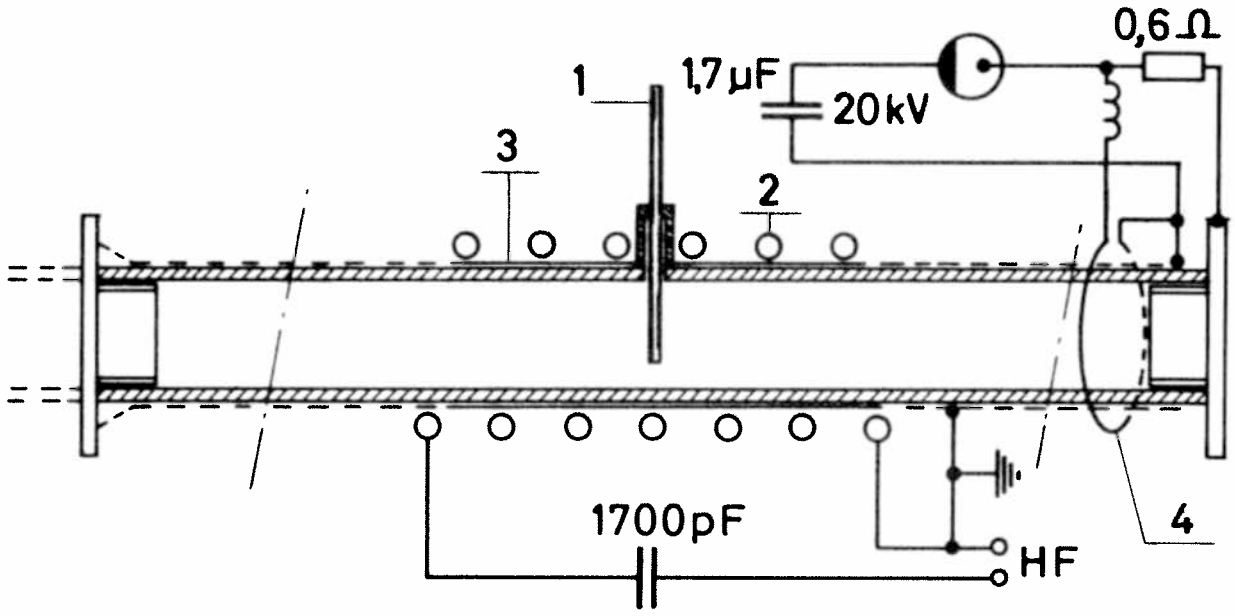

Fig. 1 Schematic diagram of experimental apparatus

1. Pressure bar
2. θ-coil
3. Split metallic screen
4. Breakdown loop for preionization discharge.

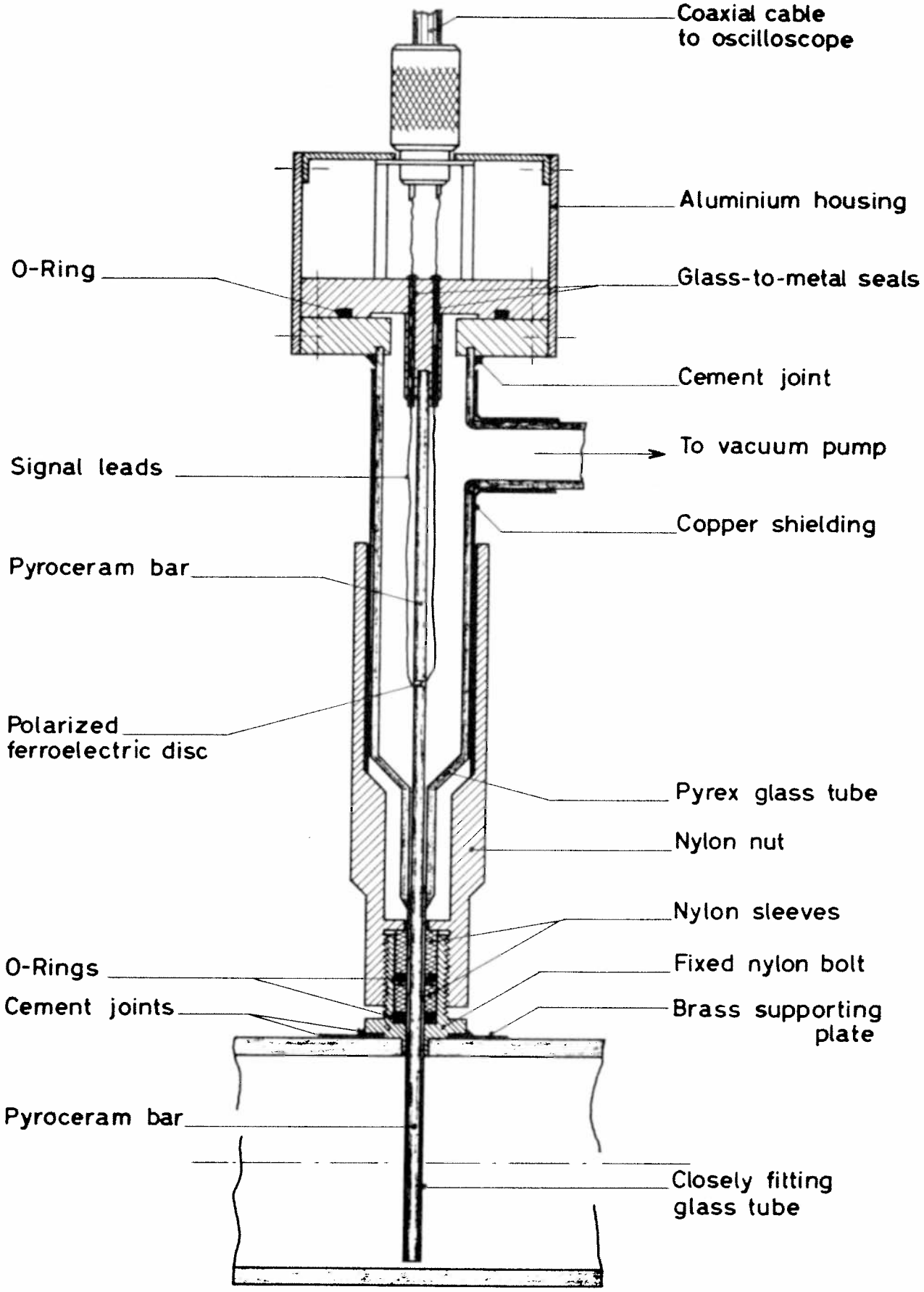

Fig. 2 Constructional details of the pressure bar and vacuum seal.

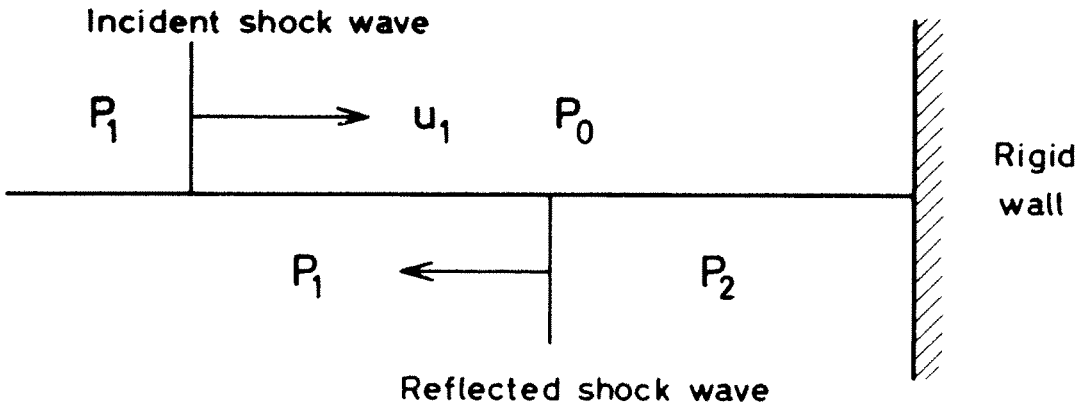

Fig. 3 Schematic representation of the reflection of a shock wave at the closed end of a shock tube.

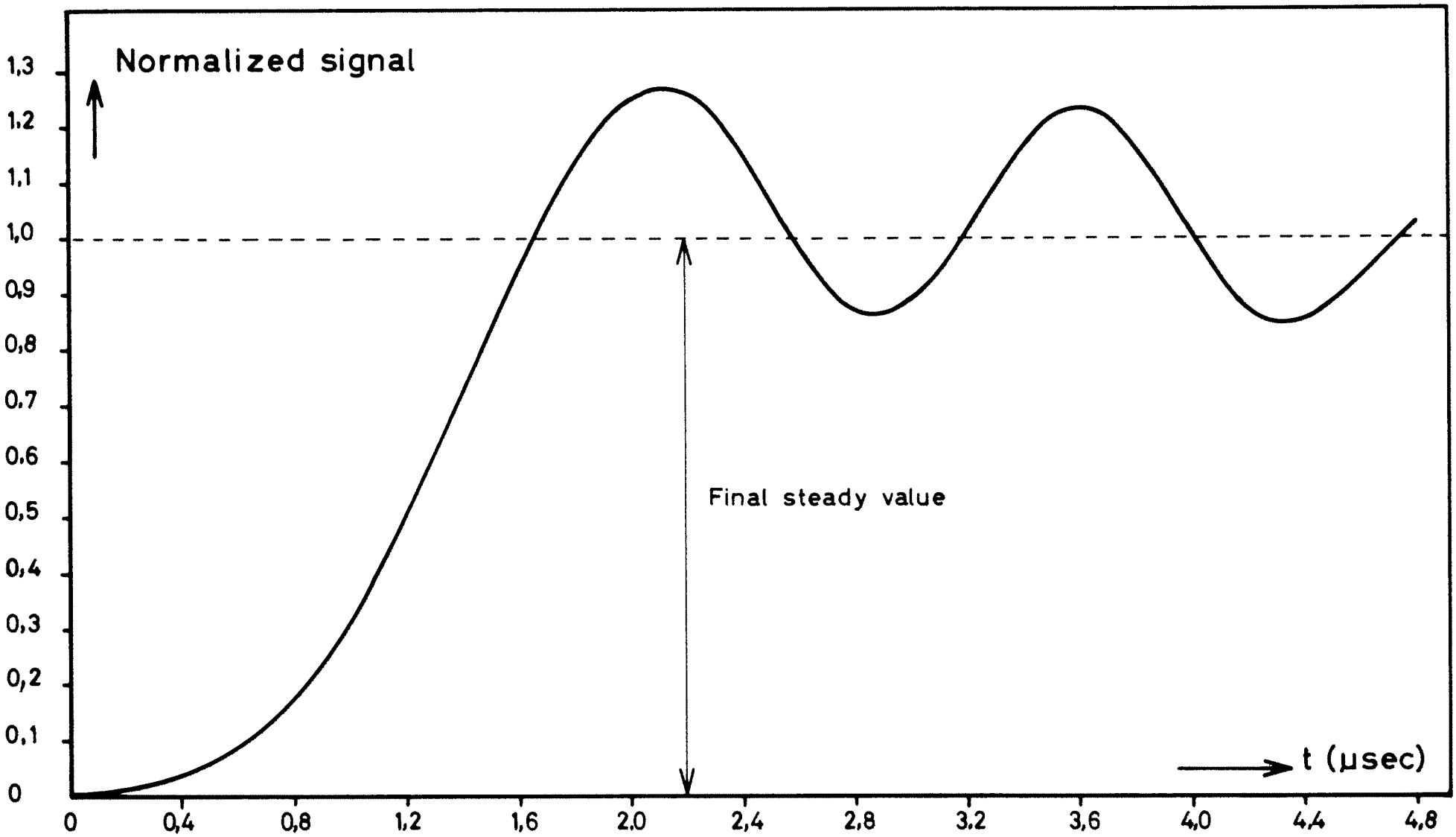

Fig. 4 Response of the pressure bar to step-pressure loading.

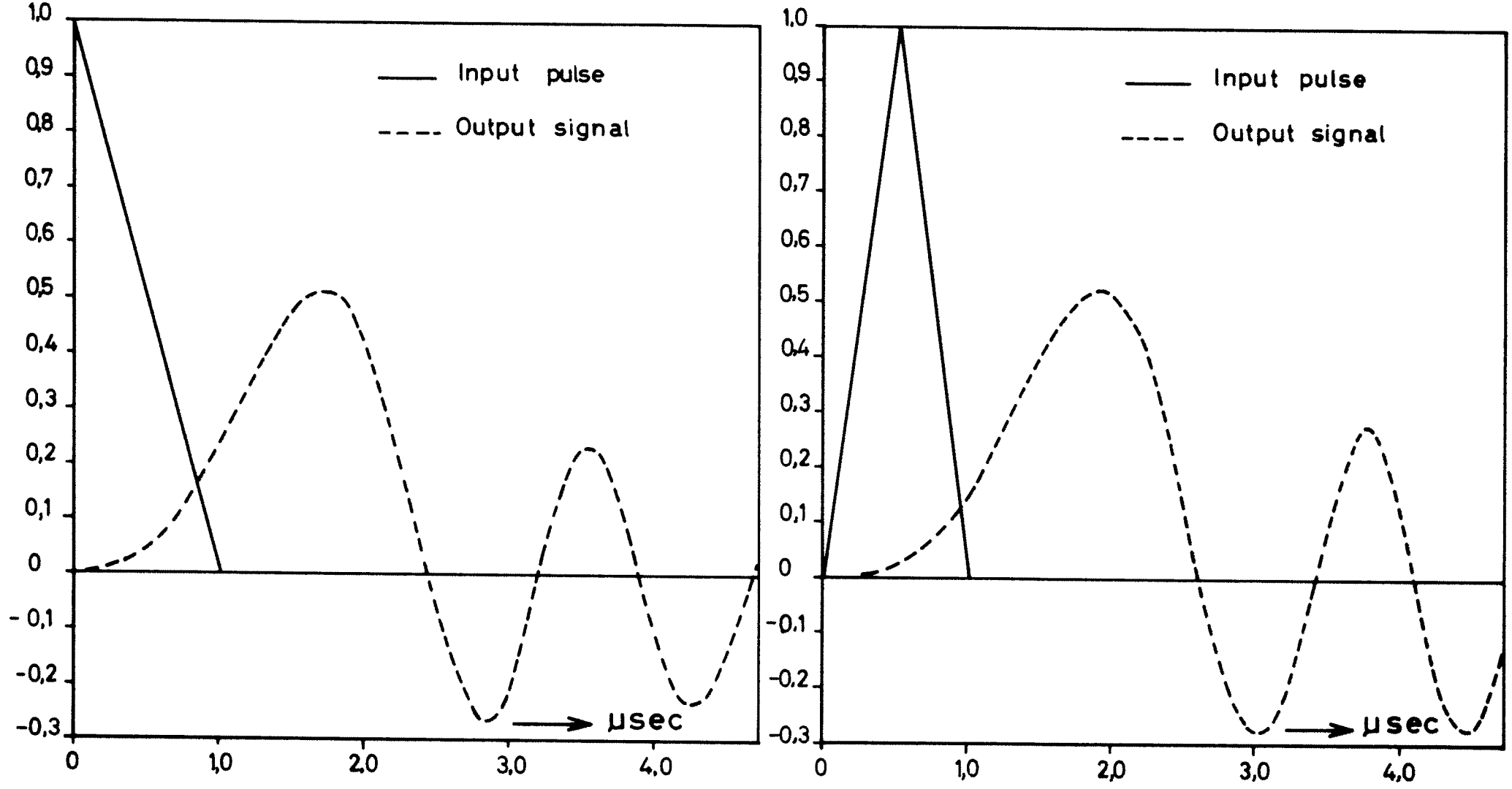

Fig. 5 Response of the pressure bar to given input pulses.

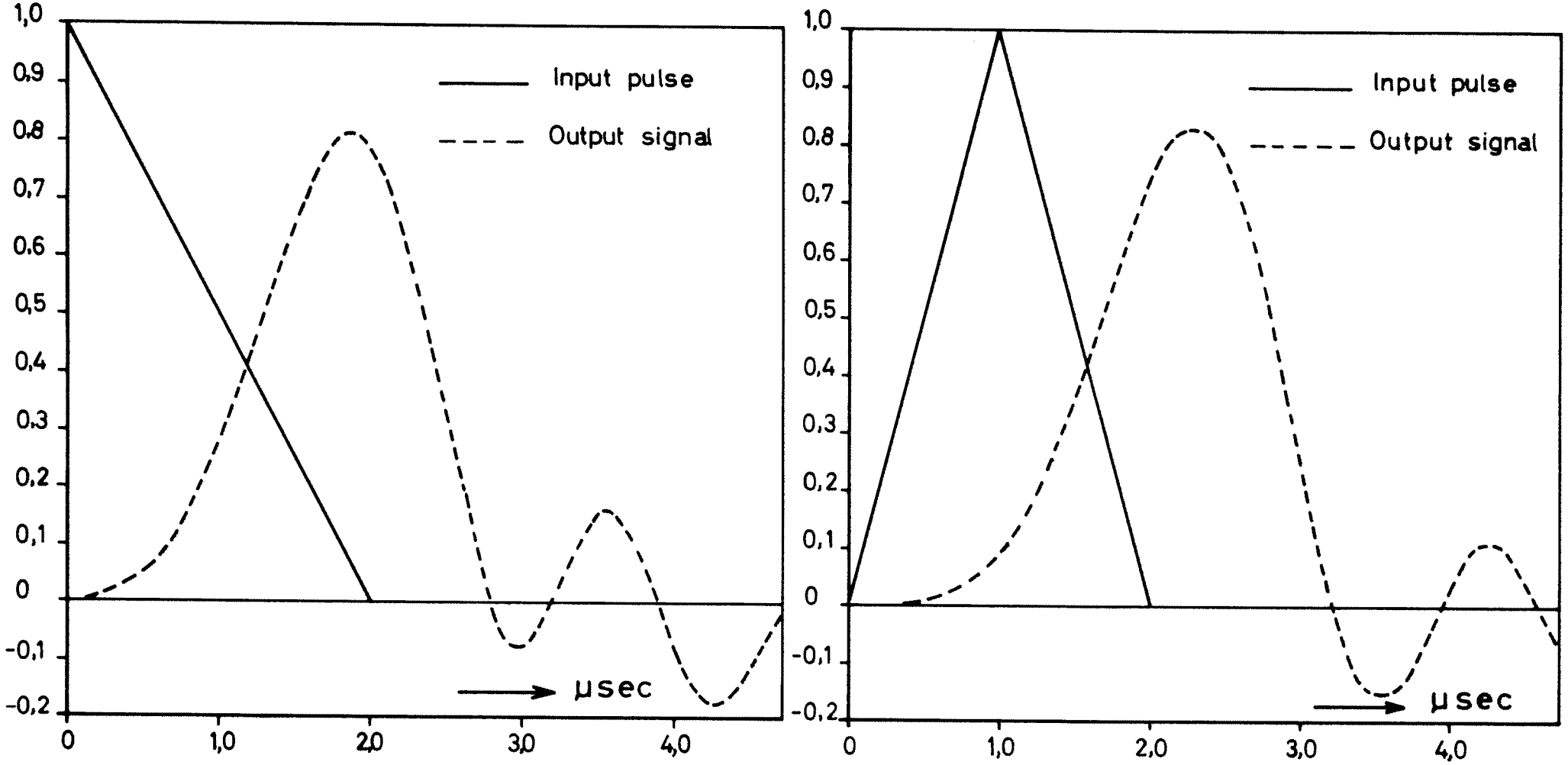

Fig. 6 Response of the pressure bar to given input pulses.

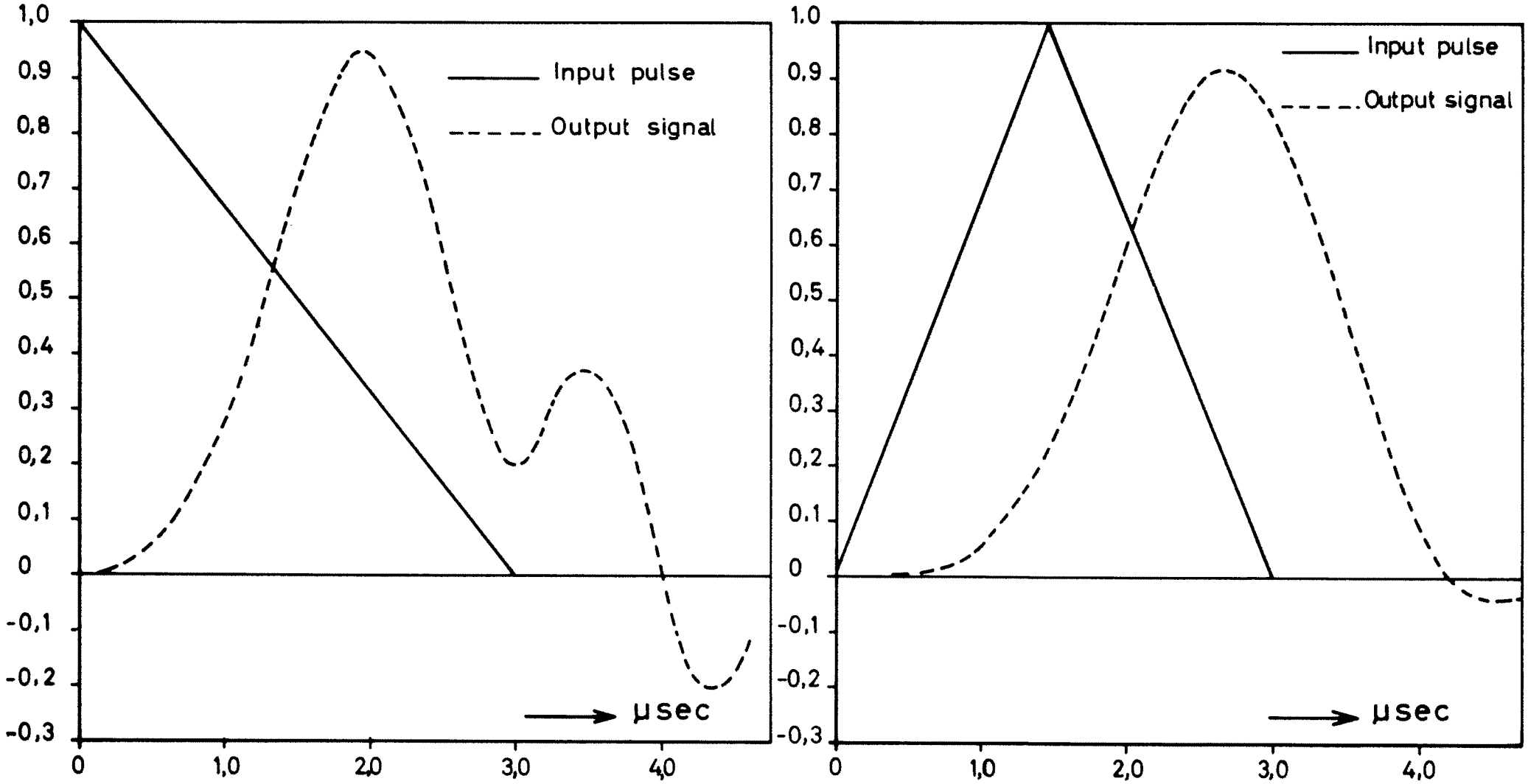

Fig. 7 Response of the pressure bar to given input pulses

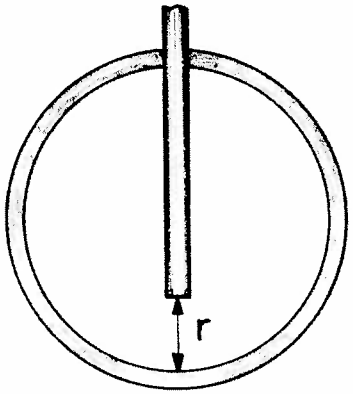

r
(mm)

$P_{(filling)}$ = 16,5 m Torr

49

26

6

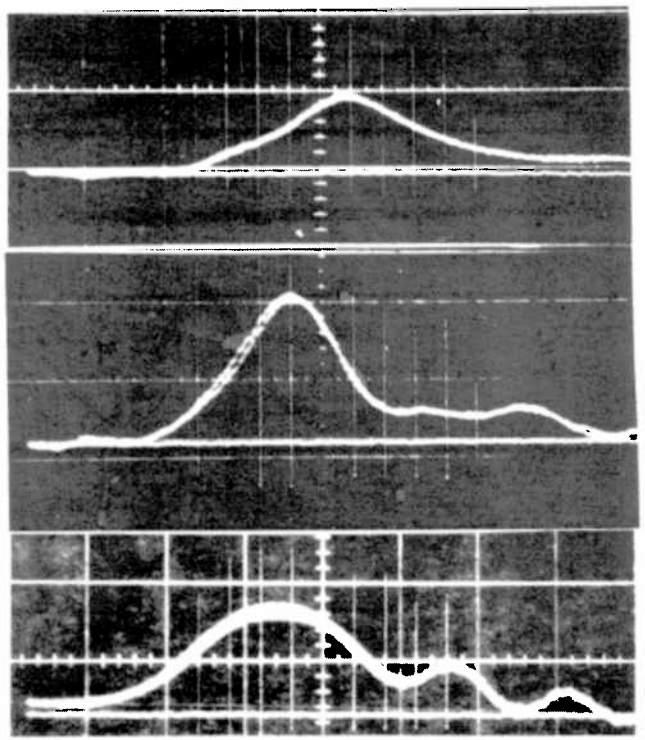

r
(mm)

$P_{(filling)}$ = 30 m Torr

49

30

12

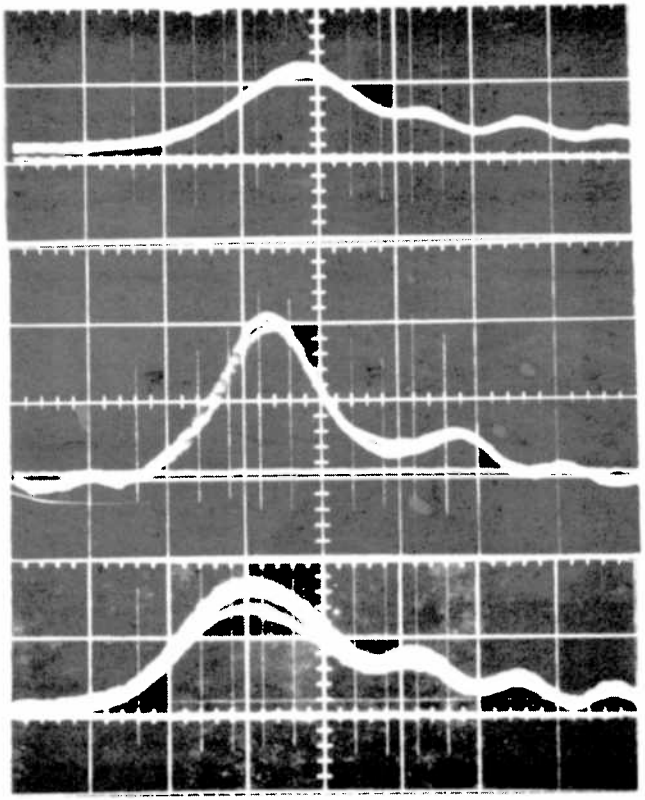

Fig. 8 Examples of pressure bar signals
(Sweep Speed : 1 μsec/div)

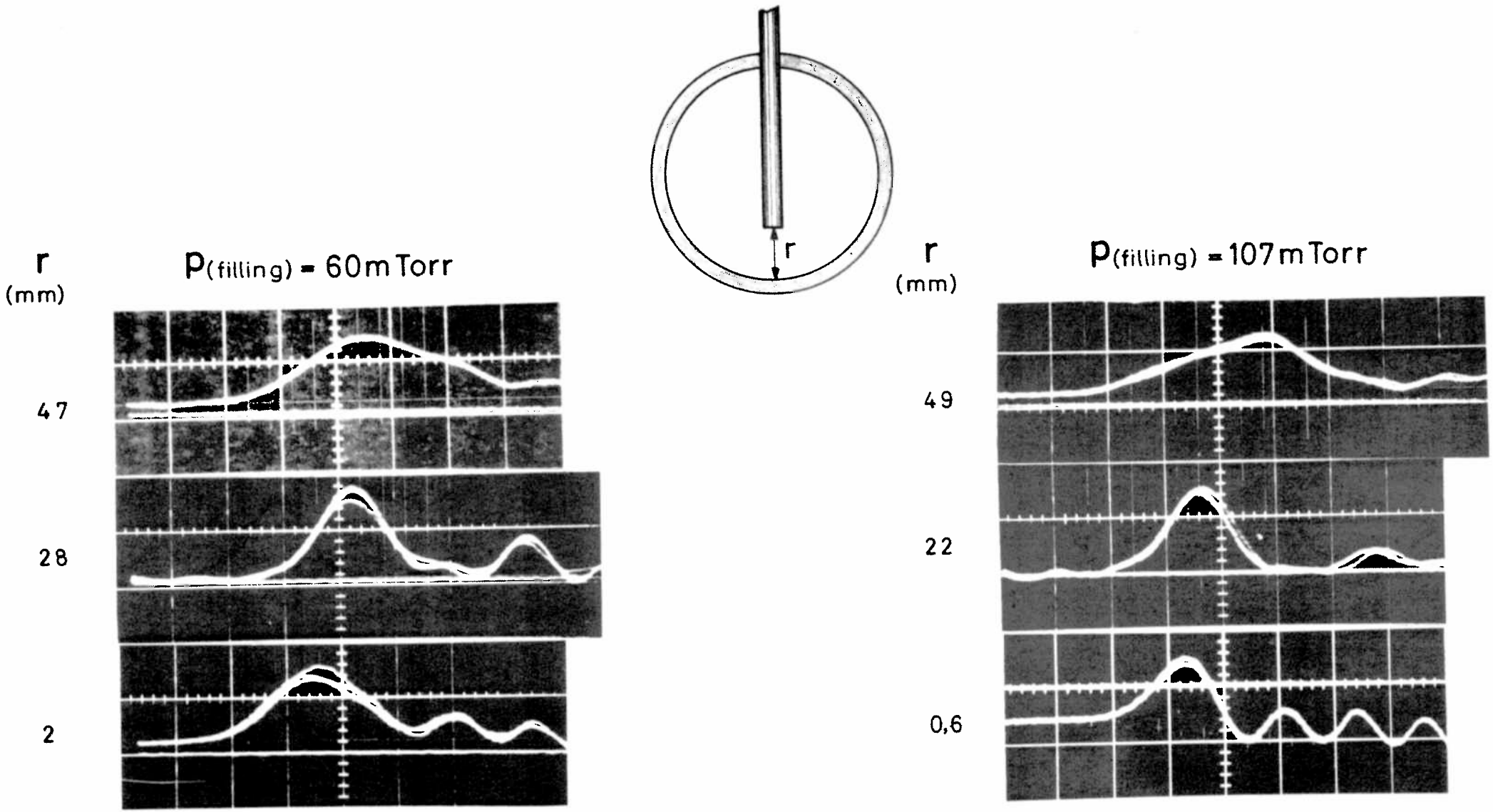

Fig. 9 Examples of pressure bar signals
(Sweep Speed : 1 μsec/div.)

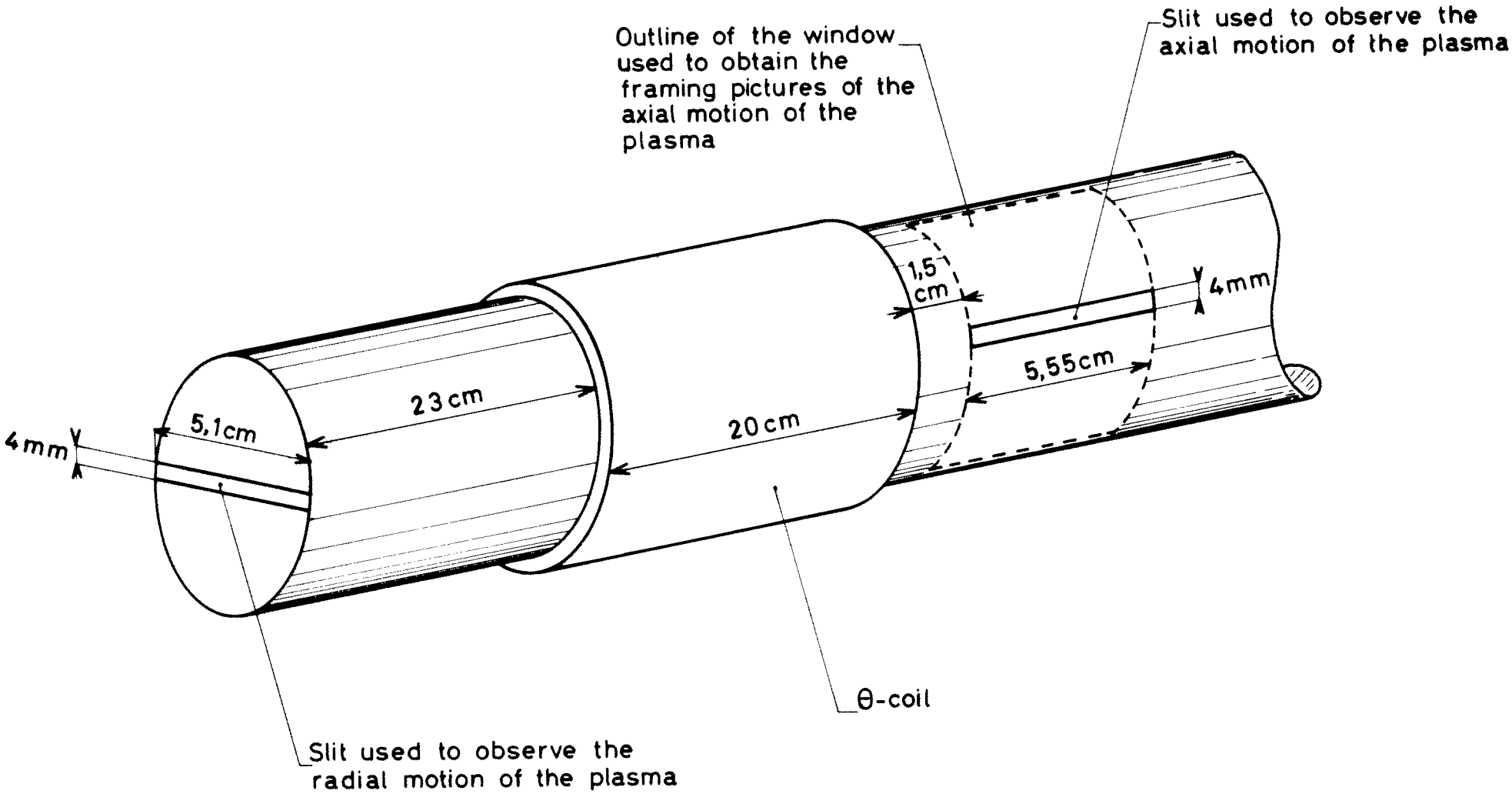

Fig. 10 The disposition and dimensions of the slits used in the photographic study.

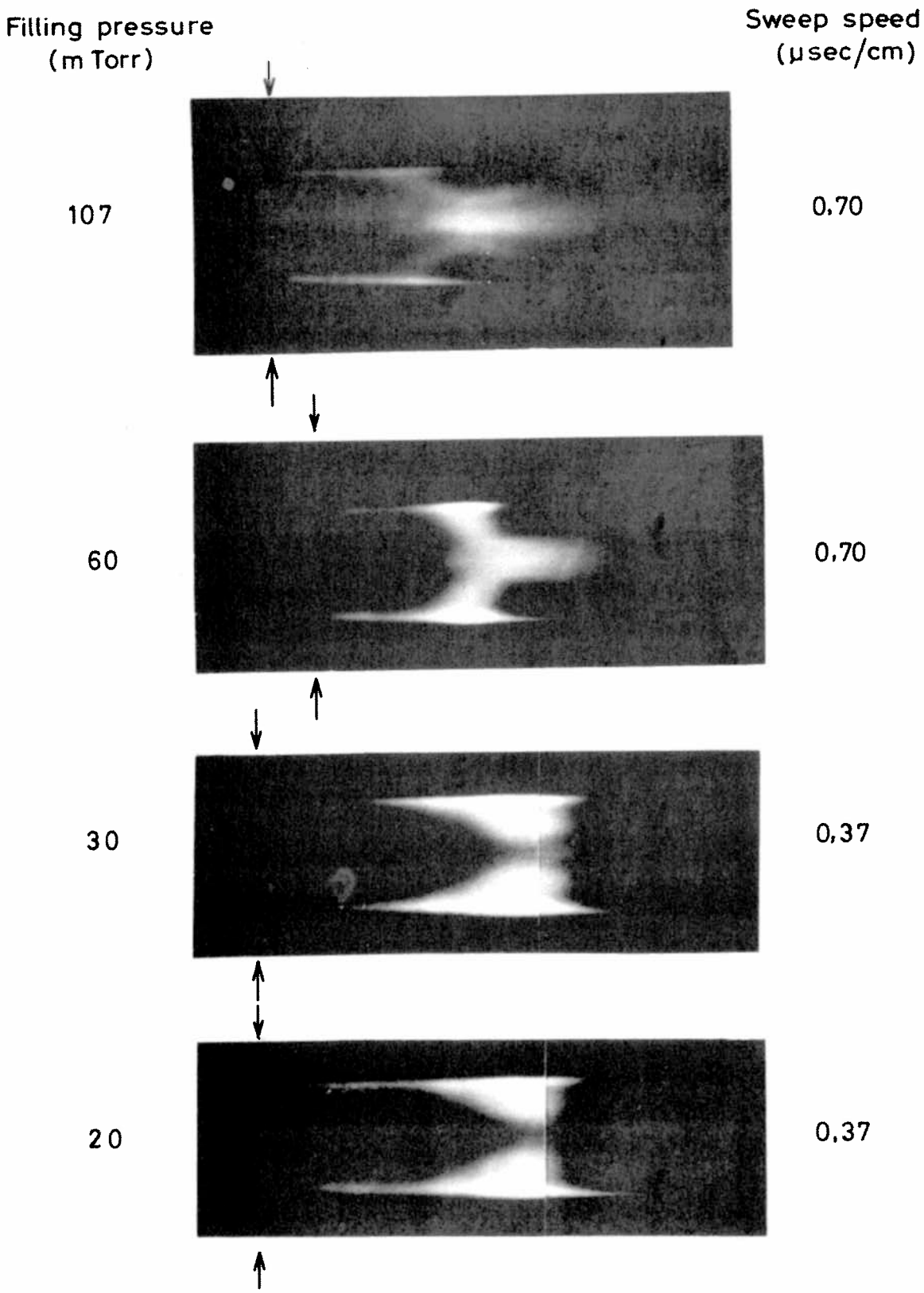

The arrows indicate the start of the high-frequency discharge. Time progresses from left to right.

Fig. 11 Streak pictures of the radial motion of the plasma.

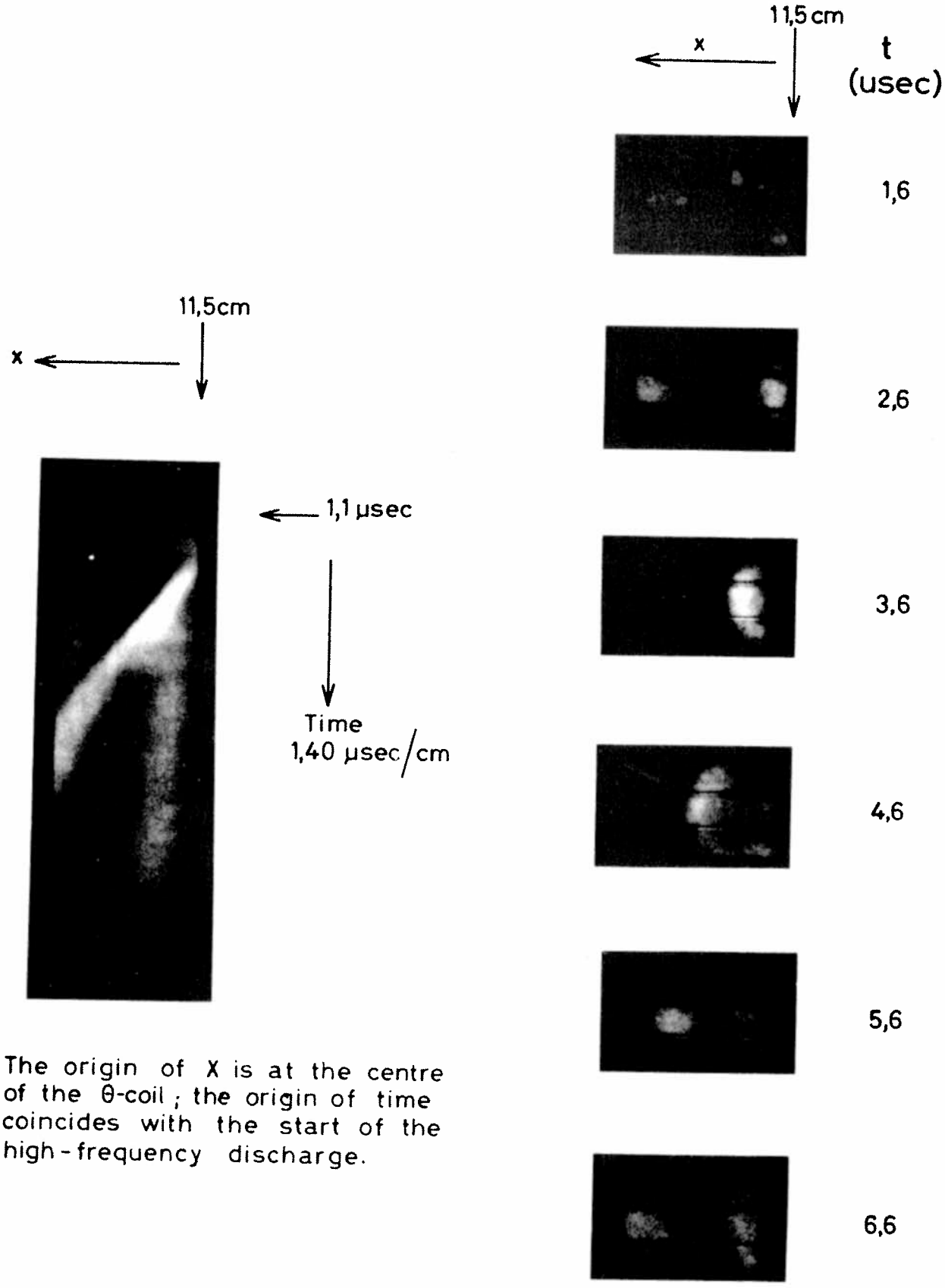

Fig. 12 Streak and frame photographs of the axial motion of the plasma.

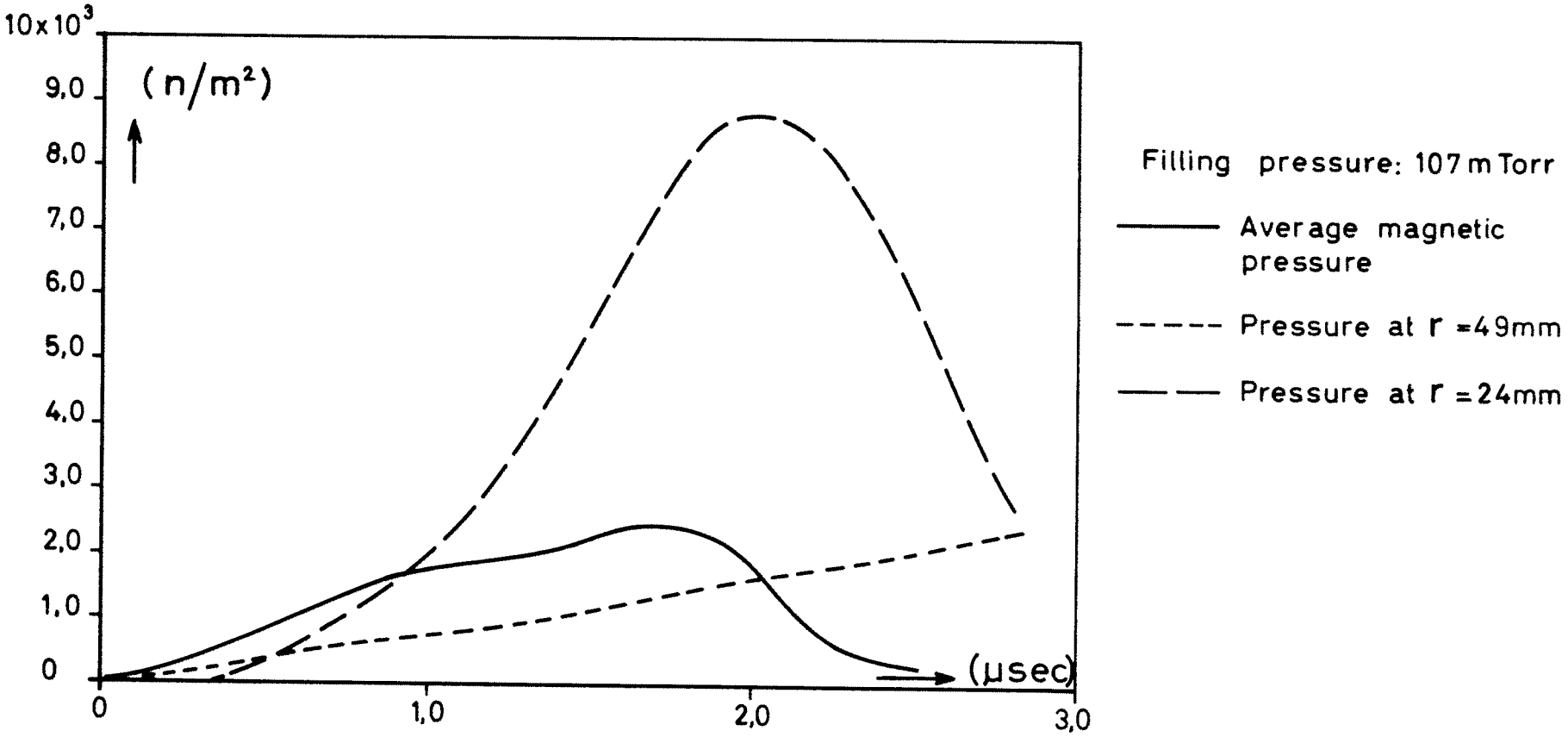

Fig. 13 Comparison of measured pressures with the average pressure of the applied magnetic field.

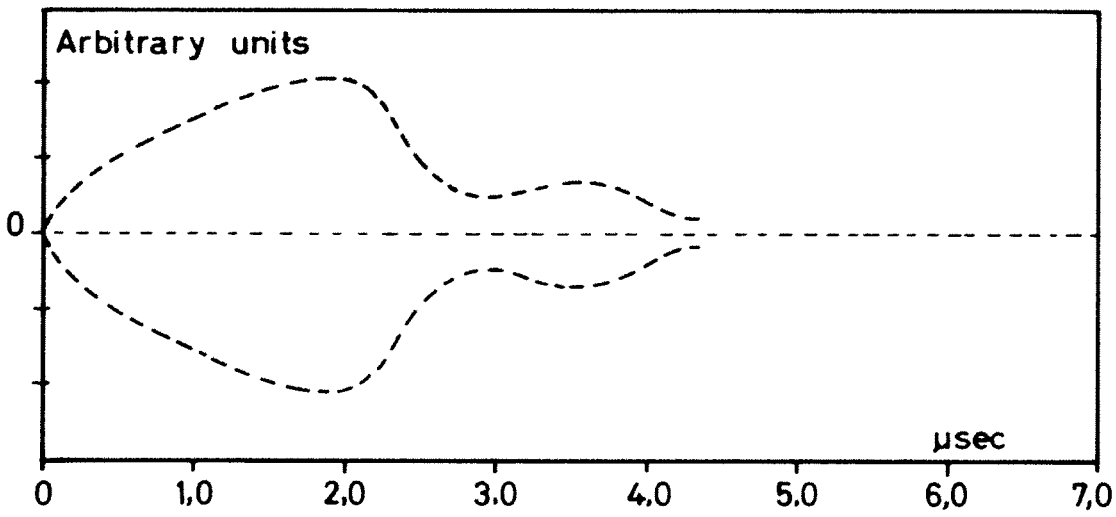

(a) Envelope of high-frequency pulse

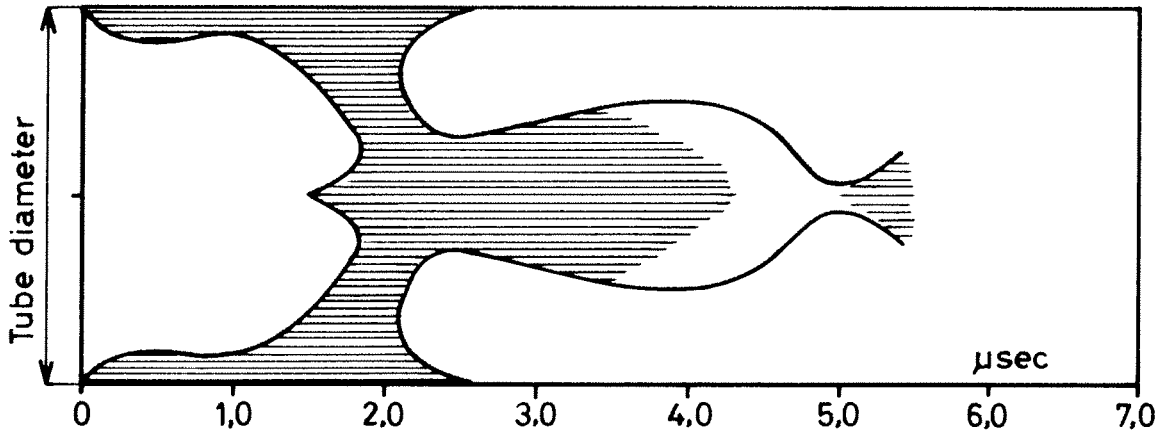

(b) Schematic representation of radial streak photograph

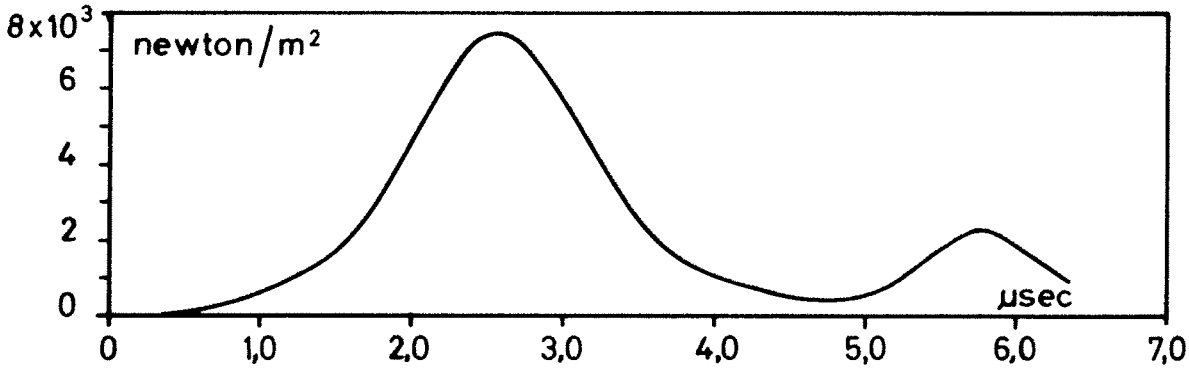

(c) Pressure bar signal at r =24mm

Filling pressure = 60 m Torr

Fig. 14 Time correlation of the high-frequency pulse, the radial streak picture and the pressure bar signal.

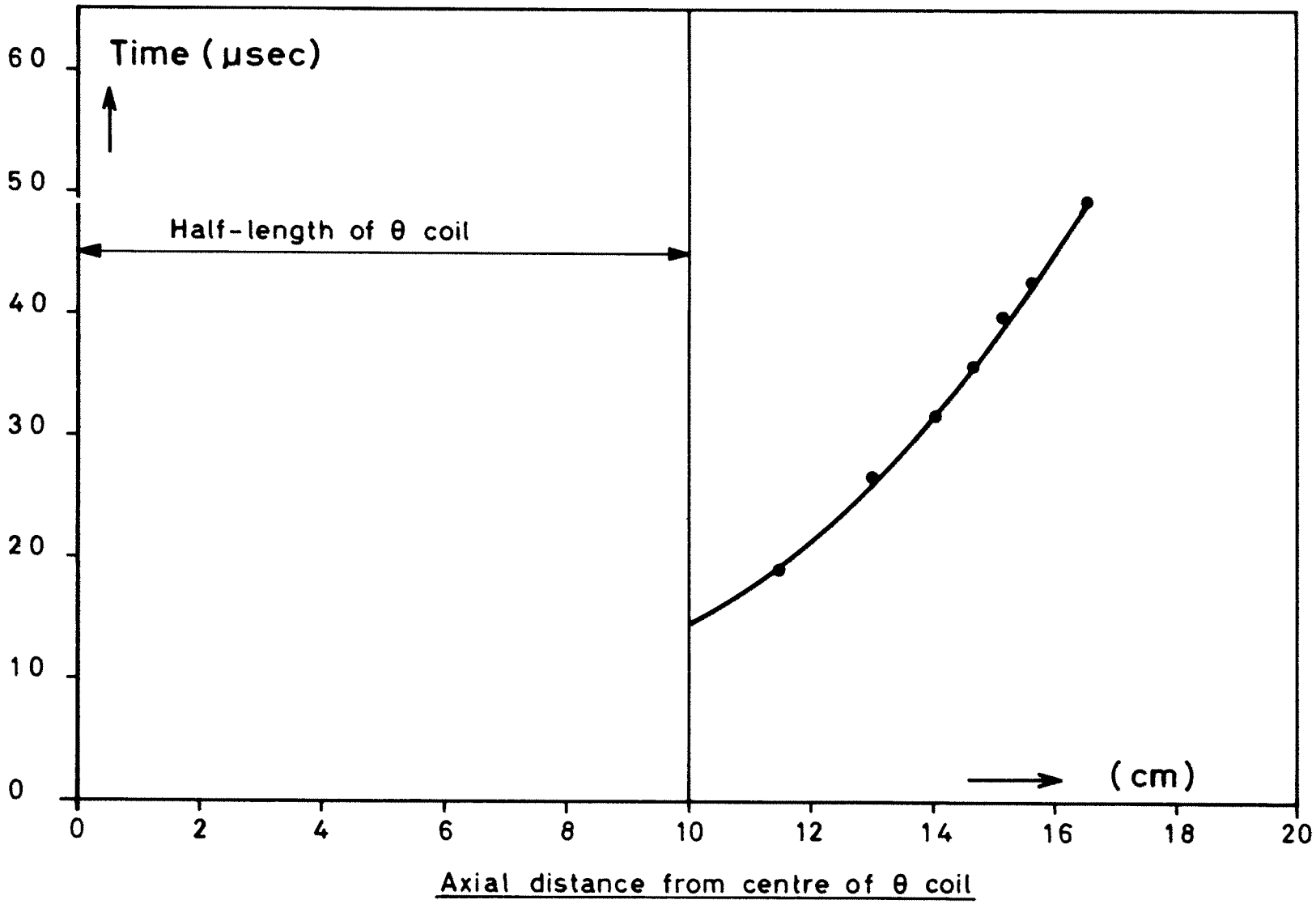

Fig. 15 x-t plot of the axial motion of the plasma; $p_{(filling)}$ = 60 mTorr.